Received: 28 February 2022 | Revised: 13 October 2022 | Accepted: 15 October 2022

DOI: 10.1111/sapm.12539

STUDIES IN APPLIED MATHEMATICS WILEY

ORIGINAL ARTICLE

Asymptotic approximation of a highly oscillatory integral with application to the canonical catastrophe integrals

Chelo Ferreira[1] | **José L. López**[2] | **Ester Pérez Sinusía**[1]

[1]Dpto. de Matemática Aplicada, IUMA, Universidad de Zaragoza, Zaragoza 50009, Spain

[2]Dpto. de Estadística, Informática y Matemáticas and INAMAT, Universidad Pública de Navarra, Pamplona 31006, Spain

Correspondence
José L. López, Dpto. Estadística, Informática y Matemáticas, Universidad Pública de Navarra, 31006-Pamplona, Navarra, Spain.
Email: jl.lopez@unavarra.es

Funding information
Universidad Pública de Navarra

Abstract

We consider the highly oscillatory integral $F(w) := \int_{-\infty}^{\infty} e^{iw(t^{K+2}+e^{i\theta}t^p)}g(t)dt$ for large positive values of w, $-\pi < \theta \leq \pi$, K and p positive integers with $1 \leq p \leq K$, and $g(t)$ an entire function. The standard saddle point method is complicated and we use here a simplified version of this method introduced by López et al. We derive an asymptotic approximation of this integral when $w \to +\infty$ for general values of K and p in terms of elementary functions, and determine the Stokes lines. For $p \neq 1$, the asymptotic behavior of this integral may be classified in four different regions according to the even/odd character of the couple of parameters K and p; the special case $p = 1$ requires a separate analysis. As an important application, we consider the family of canonical catastrophe integrals $\Psi_K(x_1, x_2, \ldots, x_K)$ for large values of one of its variables, say x_p, and bounded values of the remaining ones. This family of integrals may be written in the form $F(w)$ for appropriate values of the parameters w, θ and the function $g(t)$. Then, we derive an asymptotic approximation of the family of canonical catastrophe integrals for large $|x_p|$. The

approximations are accompanied by several numerical experiments. The asymptotic formulas presented here fill up a gap in the *NIST Handbook of Mathematical Functions* by Olver et al.

KEYWORDS
asymptotic expansions, catastrophe integrals, highly oscillatory integrals, modified saddle point method

1 | INTRODUCTION

Many short wavelength phenomena, including wave propagation and optical diffraction, may be modeled by means of mathematical theories that contain highly oscillatory integrals with several stationary phase or saddle points that are close and eventually coalesce. Uniform asymptotic approximations of those kind of integrals are often written in terms of certain canonical integrals $\Psi_K(x_1, x_2, \dots, x_K)$ denominated canonical catastrophe integrals.[2, 11] The importance of these integrals in practical applications is stressed in Ref. 10 in the following sentence: *The role played by these canonical diffraction integrals in the analysis of caustic wave fields is analogous to that played by complex exponentials in plane wave theory*.

The canonical catastrophe integrals are defined in the form Ref. 1 (Chapter 36)

$$\Psi_K(x_1, \cdots, x_K) := \int_{-\infty}^{\infty} \mathrm{e}^{\mathrm{i}\Phi_K(x_1,\cdots,x_K;u)}\mathrm{d}u, \tag{1}$$

where $\Phi_K(x_1, \dots, x_K; u)$ is a polynomial in the variable u of degree $K + 2$, denominated the cuspoid catastrophe with codimension K

$$\Phi_K(x_1, \dots, x_K; u) := u^{K+2} + \sum_{m=1}^{K} x_m u^m, \tag{2}$$

and $x_1,\dots, x_K$ are complex parameters. Integral (1) exists for either, real $x_1, \dots, x_K$; or $\Im(x_p) > 0$ and real x_m for $m = p + 1, p + 2, K$ with p even.

Apart from their applications in the uniform asymptotic approximation of oscillatory integrals,[9] these integrals have many physical applications in the description of several physical phenomena like surface gravity waves (see Refs. 8 and 12), bifurcation sets, optics, quantum mechanics, and acoustics (see Ref. 1(Section 36.14) and references therein).

A large amount of mathematical information about these integrals may be found in the reference book of special functions.[1, (Chap. 36)] Among other things, there is a classification of the integrals according to the number K of free independent parameters, the parameters that are related to the type of singularities that arise in catastrophe theory. The first three catastrophe integrals have a proper name: the simplest integral that contains only one free parameter, and that is related to the fold catastrophe, has two coalescing stationary points: it is the well-known Airy function $\Psi_1(x)$. The second integral $\Psi_2(x, y)$ is known as the Pearcey integral, contains two free parameters, is related to the cusp catastrophe, and involves three coalescing stationary points. The

third integral $\Psi_3(x,y,z)$ is known as the swallowtail integral, depends on three free parameters, corresponds to the swallowtail catastrophe, and involves four coalescing stationary points.

In Ref. 1 (Chapter 36), we can also find some symmetry properties, zeros, illustrative pictures, bifurcation sets, scaling relations, and differential equations. With respect to approximations, in Ref.1 (eq. 36.8.1), we can find the convergent expansion

$$\Psi_K(x_1,x_2,\cdots,x_K)=\frac{2}{K+2}\sum_{n=0}^{\infty}\exp\left(i\frac{\pi(2n+1)}{2(K+2)}\right)\Gamma\left(\frac{2n+1}{K+2}\right)a_{2n}(x,y,z),K\text{ even},\tag{3}$$

$$\Psi_K(x_1,x_2,\cdots,x_K)=\frac{2}{K+2}\sum_{n=0}^{\infty}i^n\cos\left(\frac{\pi(n(K+1)-1)}{2(K+2)}\right)\Gamma\left(\frac{n+1}{K+2}\right)a_{n}(x,y,z),K\text{ odd},\tag{4}$$

where $a_0(x,y,z)=1$ and, for $n=0,1,2,...,$

$$a_{n+1}(x,y,z)=\frac{i}{n+1}\sum_{p=0}^{\min(n,K-1)}(p+1)x_{p+1}a_{n-p}(x,y,z).\tag{5}$$

The convergence speed of this expansion is rather slow for moderate or large values of the variables. On the other hand, there is not much known about asymptotic approximations of these integrals for general values of K and p. In Ref. 1 (eq. 36.11.2), we can find a formal expression for the leading order approximation of $\Psi_K(x_1,x_2,\dots,x_K)$ when the variables are large, but it is valid only when the stationary points of the phase function are real and distinct, it is not an explicit analytic expression and cannot be used for numerical computations.

In Refs. 3, 4, 5, and 6, we derived complete asymptotic expansions of the second and third canonical catastrophe integrals $\Psi_2(x,y)$ and $\Psi_3(x,y,z)$ when one of their variables is large and the remaining ones are fixed. In this work, we derive an asymptotic approximation of the general canonical catastrophe integral $\Psi_K(x_1,x_2,\dots,x_K)$ for any $K\in\mathbb{N}$ and complex $x_1,\dots,x_K$, when one of its variables, say x_p, is large and the remaining ones are fixed. The analysis here is more complicated that the one of the previously mentioned references. It requires a detailed study of the steepest descent paths and saddle points of the phase function, and the admissible deformations of the integration contour. The location of these paths and saddle points and the deformation of the integration contour strongly depend on the form of the phase function. These essential ingredients of the analysis cannot be inferred from the particular cases $K=2$ or $K=3$ analyzed so far. There, the study was more or less straightforward as the phase function is a specific function. Now the analysis is much more involved as we must find steepest descent paths, saddle points, and admissible deformations for the whole family of phase functions at once. These elements strongly depend on K, p, and the phase of x_p. As a consequence, the complex x_p-plane is divided in different asymptotic regions separated by Stokes lines. Because of the complexity of the analysis, we derive only the dominant term of the asymptotic expansion of $\Psi_K(x_1,x_2,\dots,x_K)$ in inverse powers of x_p. To accomplish this task, we consider the more general highly oscillatory integral

$$F(w):=\int_{-\infty}^{\infty}\mathrm{e}^{iw(u^{K+2}+e^{i\theta}u^p)}g(u)\mathrm{d}u\tag{6}$$

for large positive values of w, with $-\pi<\theta\le\pi$, K and p positive integers satisfying $1\le p\le K$, and $g(u)$ an entire function. The canonical catastrophe integrals (1) are a particular case of this integral for appropriate values of the parameters w,θ and the function $g(t)$. The key point in our

analysis is the derivation of the asymptotic behavior of the integral (6). Then, as an application, we derive the asymptotic behavior of the family of canonical catastrophe integrals (1).

The asymptotic analysis of $F(w)$ is carried out in Sections 2–5. In Section 2, we rotate the integration interval $(-\infty, \infty)$ to avoid the strong oscillations of the integrand. In Section 3, we find the saddle points of the integral $F(w)$ and determine the *simplified* steepest descent paths of the *simplified* saddle point method introduced in Ref. 7. In Section 4, we compute the asymptotic approximation of the integrals over the simplified steepest descent paths. In Section 5, we analyze the relevant saddle points and the deformation of the integration path to the relevant simplified steepest descent paths. This analysis strongly depends on the even/odd character of K and p; therefore, we analyze every case separately in different subsections. In Section 6, we apply the results of the previous sections to derive an asymptotic approximation of the family of the catastrophe integrals $\Psi_K(x_1, x_2, \dots, x_K)$ for one large parameter x_p in terms of elementary functions. This approximation is given in formulas (36)–(37), complemented with some details about the Stokes lines in Table 1, and illustrated in Figures 23–26. The asymptotic approximation (36)–(37) is illustrated in Section 7 by means of some numerical experiments. Throughout all the paper, we use the principal argument $\arg z \in (-\pi, \pi]$ for any complex number z and the notation z^* for the complex conjugate of z.

2 | PRELIMINARIES

The integral (6) is not appropriate for an asymptotic analysis because of the highly oscillatory character of the integrand. Then, we deform the integration contour $(-\infty, \infty)$ to another contour where the integrand decays exponentially. The deformation is different for even and odd K. For even K, we rotate the path $(-\infty, \infty)$ an angle $\alpha := \frac{\pi}{2(K+2)}$. Then, integral (6) may be written in the form

$$F(w) = \int_{C_e} \mathrm{e}^{iw(t^{K+2} + e^{i\theta} t^p)} g(t) \mathrm{d}t, \tag{7}$$

with $C_e := (-e^{i\alpha}\infty, e^{i\alpha}\infty)$.

For odd K, we split the integration interval $(-\infty, \infty)$ at $u = 0$ and rotate the path $(-\infty, 0)$ an angle $\pi - \alpha$, and the path $(0, \infty)$ an angle α. Then, integral (6) may be written in the form

$$F(w) = \int_{C_o} \mathrm{e}^{iw(t^{K+2} + e^{i\theta} t^p)} g(t) \mathrm{d}t, \tag{8}$$

with $C_o := (e^{i(\pi-\alpha)}\infty, 0] \cup [0, e^{i\alpha}\infty)$. The paths C_e and C_o are depicted in Figure 1. Integrals (7) and (8) are absolutely convergent for entire functions $g(t)$ that do not grow faster than $t^{-1-\varepsilon}\mathrm{e}^{w|t|^{K+2}}$, $\varepsilon > 0$, when $|t| \to \infty$.

3 | SADDLE POINTS AND SIMPLIFIED STEEPEST DESCENT PATHS

Consider the change of integration variable $u \to t$ in (1) defined in the form $u = |x_p|^\sigma t$, with

$$\sigma := \frac{1}{K + 2 - p}. \tag{9}$$

TABLE 1 Values of the parameter β and the sectors R_e, R_p in formula (37), together with the corresponding Stokes lines of the asymptotic approximation (36)–(37) of $\Psi_K(x_1, x_2, \dots, x_K)$ for large $|x_p|$

		$\boldsymbol{\beta}$	$\boldsymbol{R_e}$	$\boldsymbol{R_p}$	**Stokes lines ($\theta =$)**
$p = 1$	K even	σ for $-\pi < \theta \le -\frac{\pi}{2(K+2)}$			
		$\sigma(K+1)$ for $-\frac{\pi}{2(K+2)} < \theta \le \frac{(2K+3)\pi}{2(K+2)}$	$(-\pi, \pi]$	$\emptyset$	$0, \pi, -\frac{\pi}{K+2}, \frac{(K+1)\pi}{K+2}$
		$\sigma(2K+1)$ for $\frac{(2K+3)\pi}{2(K+2)} < \theta \le \pi$			
	K odd	σ for $-\pi < \theta \le 0$	$(-\pi, \pi]$	$\emptyset$	$\pi, -\frac{\pi}{K+2}, \frac{\pi}{K+2}$
		σK for $0 < \theta \le \pi$			
K even	p even	σ for $K = p$	$(-\pi, -\frac{p\pi}{K+2}]$	$(-\frac{p\pi}{K+2}, \pi]$	$\pi, -\frac{p\pi}{K+2}$
		$\sigma(K+3-p)$ for $K \ne p$			
	p odd $\ne 1$	σ for $-\pi < \theta \le -\frac{p\pi}{K+2}$	$(-\pi, -\frac{p\pi}{K+2}] \cup [0, \frac{\pi}{\sigma(K+2)}]$	$(-\frac{p\pi}{K+2}, 0] \cup (\frac{\pi}{\sigma(K+2)}, \pi]$	$0, \pi, -\frac{p\pi}{K+2}, \frac{(K+2-p)\pi}{K+2}$
		1 for $0 \le \theta \le \frac{\pi}{\sigma(K+2)}$			
K odd	p even, $2p < K+2$	σ for $-\pi < \theta \le \frac{-p\pi}{K+2}$	$(-\pi, \frac{-\pi}{\sigma(K+2)}] \cup [\frac{-\pi}{\sigma(K+2)}, \frac{-p\pi}{K+2}] \cup (\frac{-p\pi}{K+2}, 0]$	$[0, \pi]$	$0, \pi$
		1 for $\frac{-p\pi}{K+2} < \theta \le 0$			
	p even, $2p > K+2$	σ for $-\pi < \theta \le \frac{-p\pi}{K+2}$	$(-\pi, \frac{-p\pi}{K+2}] \cup [\frac{-\pi}{\sigma(K+2)}, 0]$	$[\frac{-p\pi}{K+2}, \frac{-\pi}{\sigma(K+2)}] \cup [0, \pi]$	$0, \pi, -\frac{p\pi}{K+2}, \frac{(p-K-2)\pi}{K+2}$
		1 for $\frac{-\pi}{\sigma(K+2)} \le \theta \le 0$			
	p odd $\ne 1$	σ for $-\pi < \theta \le \frac{-p\pi}{K+2}$	$(-\pi, \frac{-p\pi}{K+2}] \cup [\frac{p\pi}{K+2}, \pi]$	$[\frac{-p\pi}{K+2}, \frac{p\pi}{K+2}]$	$\pi, -\frac{p\pi}{K+2}, \frac{p\pi}{K+2}$
		$\sigma(K-p+1)$	for $\frac{p\pi}{K+2} \le \theta \le \pi$		

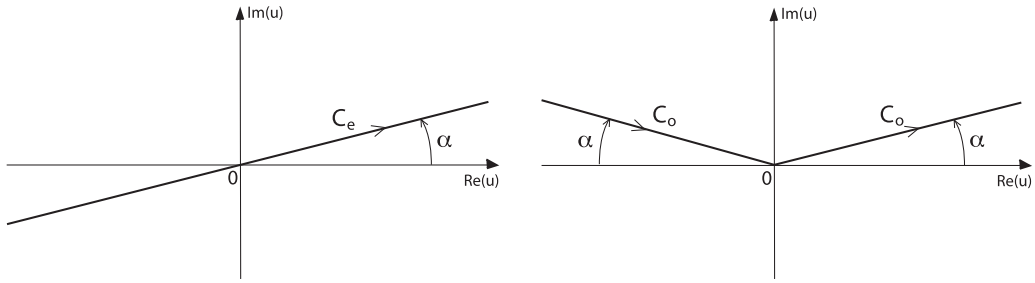

FIGURE 1 Integration path C_e in (7) (left picture) and integration path C_o in (8) (right picture)

With this change of variable, we find that, apart from a factor $|x_p|^\sigma$, the catastrophe integrals (1) may be written in the form (7) (for even K) or (8) (for odd K) with $w = |x_p|^{(K+2)\sigma}$, $\theta = \arg x_p$, and

$$g(t) = \exp\{i \sum_{\substack{m=1 \\ m\neq p}}^{K} x_m (|x_p|^\sigma t)^m\}. \tag{10}$$

Although it is possible to do an asymptotic analysis for integrals (7) and (8) for general entire functions $g(t)$, for the sake of simplicity, we specialize here on this particular family of functions $g(t)$.

Either from the simplified version of the saddle point method,[7] or from the standard steepest descent method,[13, (Chap. 2)] it is clear that the phase function in either (7) or (8) is the function

$$f(t) := t^{K+2} + e^{i\theta} t^p. \tag{11}$$

From Ref. 7, we know that the presence of the large parameter $|x_p|$, not only in front of the phase function $f(t)$ (the parameter $w = |x_p|^{(K+2)\sigma}$ in (7) or (8)), but also in the function $g(t)$ does not spoil the asymptotic analysis. Essentially, this is so because the power of $|x_p|$ in front of the phase function $f(t)$ is larger than the powers of $|x_p|$ in the different summands of the exponent of $g(t)$ in (10) (see Ref. 7 for further details).

For any value of p, the $K - p + 2$ points

$$t_n := \left(\frac{p}{K+2}\right)^\sigma e^{i\sigma[\theta+(2n+1)\pi]}, n = 0, 1, \cdots, K - p + 1, \tag{12}$$

are saddle points of the phase function $f(t)$ of multiplicity one. They are located on a circle of center the origin and radius $(\frac{p}{K+2})^\sigma$, and are angularly equally spaced. But, moreover, for $p > 1$, the origin $t_{K-p+2} := 0$ is also a saddle point of multiplicity $p - 1$.

Either from the simplified version of the saddle point method,[7] or from the standard steepest descent method,[13, (Chap. 2)] we know that the asymptotically relevant saddle points are those ones for which the integration path C_e in (7) or C_o in (8) can be deformed into a simplified steepest descent path (or union of simplified steepest descent paths) that contains the dominant saddle points. We have carried out this analysis in our previous papers,[3–6] for $K = 4$ and $K = 5$ and specific values of p. Now, for general values of p and K, the analysis requires a more detailed study and strongly depends on the odd/even character of K and p.

The analytic expression of the steepest descent paths of $f(t)$ at the saddle points is not straightforward. But we know from Ref. 7 that the asymptotic analysis of the integrals (7) of (8) does not require the computation of the steepest descent paths of $f(t)$ at the relevant saddle points t_n, but just its simplified steepest descent paths, which are nothing but the standard steepest descent paths of the "main part" of the phase function $f(t)$ at the relevant saddle points t_n. These simplified steepest descent paths may always be computed in a straightforward manner, as they are nothing but straight lines.[7] Their particular form depends on the multiplicity m of the saddle point: $m = 1$ for $n = 0, 1, \dots, K - p + 1$ and $m = p - 1$ for $n = K - p + 2$.

Following the notation of Ref. 7, at every saddle point t_n, we denote by ϕ_n the phase of $f^{(m+1)}(t_n)$ and by $f_{m+1}(t)$ the Taylor polynomial of degree $m + 1$ of $f(t)$ at the saddle point: $f_{m+1}(t) := f(t_n) + f^{(m+1)}(t_n)(t - t_n)^{m+1}/(m + 1)!$ At every steepest descent straight line, the "main part" of $f(t)$ is just $f_{m+1}(t)$ and, at each saddle point t_n, $n = 0, 1, 2, \dots, K - p + 2$, we have that the simplified steepest descent paths of $f_{m+1}(t)$ are the following straight lines emanating from the saddle points:[7]

$$\Gamma_{n,s} = \left\{ t_n + re^{i\theta_{n,s}}; \theta_{n,s} = \frac{(2s+1)\pi - \phi_n}{m+1}; 0 < r < \infty \right\}, s = 0, 1, 2, \cdots, m. \tag{13}$$

Then, the first point of the asymptotic analysis of (7) and (8) is the computation of the simplified steepest descent paths of $f_{m+1}(t)$. For our phase function $f(t) := t^{K+2} + e^{i\theta}t^p$, we have that $f''(t) = (K + 2)(K + 1)t^K + p(p - 1)e^{i\theta}t^{p-2}$. Then, at the saddle points t_n, $n = 0, 1, \dots, K - p + 1$, the first nonvanishing derivative is the second one, which means $m = 1$ and, for $n = 0, 1, \dots, K - p + 1$,

$$f(t_n) = \frac{p - K - 2}{K + 2}\left(\frac{p}{K+2}\right)^{\sigma p} e^{i\sigma(K+2)[\theta+(2n+1)\pi]}, \tag{14}$$

$$f''(t_n) = p(K + 2 - p)\left(\frac{p}{K+2}\right)^{\sigma(p-2)} e^{i\sigma K[\theta+(2n+1)\pi]}. \tag{15}$$

On the other hand, at the saddle point $t_{K-p+2} = 0$, the first nonvanishing derivative is the p-th derivative, with $p \geq 2$, which means $m = p - 1$ and $f(0) = 0$, $f^{(p)}(0) = p!e^{i\theta}$.

Now we can write the precise form of the simplified steepest descent paths $\Gamma_{n,s}$ at every saddle point t_n of $f_{m+1}(t)$ derived from formula (13). At $t = t_n$, $n = 0, 1, \dots, K - p + 1$, we have that there are two steepest descent paths $\Gamma_{n,s}$, $s = 0, 1$, that are given by formula (13) with

$$\phi_n = K\sigma[\theta + (2n + 1)\pi] + \frac{\pi}{2} \Rightarrow \theta_{n,s} = s\pi - \frac{K[\theta + (2n + 1)\pi]}{2(K - p + 2)} + \frac{\pi}{4}, s = 0, 1. \tag{16}$$

On the other hand, at $t = 0$, we have that there are p steepest descent paths $\Gamma_{K+2-p,s}$, $s = 0, 1, \dots, p - 1$, which are given by formula (13) with

$$\phi_{K+2-p} = \theta + \frac{\pi}{2} \Rightarrow \theta_{K-p+2,s} = \frac{(2s + 1/2)\pi - \theta}{p}, s = 0, 1, \cdots, p - 1. \tag{17}$$

The relevant saddle points that determine the deformation of the integration path to the corresponding union of simplified steepest descent paths $\Gamma_{n,s}$ and then the asymptotic behavior are analyzed in Section 5. To finish this section, we determine the dominant saddle points, that is, those ones for which $\Re(f(t_n))$ is maximum, which is necessary for the analysis of Section 5. This, of course, depends on K, p and the argument θ of the asymptotic variable x_p. We have

that $f(0) = 0$ and $\Re(f(t_n)) = \cos[\sigma(K+2)[\theta + (2n+1)\pi] + \pi]$ for $0, 1, 2, \dots, K+1-p$. Therefore, the dominant saddle point is the point t_{n^*}, where n^* is the value of n at which the following maximum is attained:

$$\max_{n\in\{0,1,\dots,K+2-p\}} \begin{cases} 0, & \text{if } n = K+2-p, \\ \cos\left[\dfrac{(K+2)[\theta+(2n+1)\pi]}{K+2-p} + \dfrac{3\pi}{2}\right], & \text{if } n = 0, 1, 2, \dots, K+1-p. \end{cases} \tag{18}$$

4 | INTEGRALS OVER THE SIMPLIFIED STEEPEST DESCENT PATHS

In this section, we compute the asymptotic approximation of the integrals (7) and (8) over any of the steepest descent paths $\Gamma_{n,s}$ defined in (13), with $\theta_{n,s}$ given in (16) and (17).

The multiplicity of the saddle points $t_{K+2-p} = 0$ is p, and then the simplified steepest descent path through this point is the union of two paths $\Gamma_{K+2-p,s}$ for a certain couple of values of the parameter $s = 0, \dots, p-1$, that we do not know at this moment; therefore, we compute below, in Section 4.1, the integral over all the paths $\Gamma_{K+2-p,s}$ and later, in the next section, we will determine the precise couple of values of s to be used in the asymptotic approximation. On the other hand, the multiplicity of the saddle points t_n, $n = 0, \dots, K+1-p$, is two, and then the simplified steepest descent path through these points is always $\Gamma_{n,0} \cup \Gamma_{n,1}$; therefore, we compute below, in Section 4.2, the integral over the union $\Gamma_{n,0} \cup \Gamma_{n,1}$.

4.1 | Integrals over the steepest descent paths at the origin

The integrals over the simplified steepest descent paths $\Gamma_{K+2-p,s}$, $s = 0, 1, 2, \dots, p-1$, at $t = t_{K-p+2} = 0$ are

$$F_0^s(x_1, \cdots, x_K) := |x_p|^\sigma \int_{\Gamma_{K+2-p,s}} \mathrm{e}^{\mathrm{i}|x_p|^{(K+2)\sigma} e^{i\theta} t^p} g_0(x_1, \cdots, x_K; t) dt, s = 0, 1, 2, \cdots, p-1, \tag{19}$$

with

$$g_0(x_1, \dots, x_K; t) := \exp\left[\mathrm{i}|x_p|^{(K+2)\sigma} e^{i\theta} t^{K+2} + \mathrm{i} \sum_{m=1, m\neq p}^{K} x_m (|x_p|^\sigma t)^m\right], \tag{20}$$

$$t = e^{\mathrm{i}[(2s+1/2)\pi - \theta]/p} u, 0 \le u < \infty. \tag{21}$$

Following Ref. 7, the asymptotic approximation of $F_0^s(x_1, \dots, x_K)$ for large $|x_p|$ is obtained after the change of variable $t \to t|x_p|^{-(K+2)\sigma/p}$, and replacing $g_0(x_1, \dots, x_K; t)$ by $g_0(x_1, \dots, x_K; 0) = 1$. Then,

$$F_0^s(x_1, \dots, x_K) = \frac{\Gamma\left(1 + \frac{1}{p}\right)}{x_p^{1/p}} e^{i\pi/(2p)} e^{i\pi s} \left[1 + \mathcal{O}\left(\frac{1}{x_p^{1/p}}\right)\right]. \tag{22}$$

4.2 | Steepest descent paths at t_n, $n = 0, 1, \dots, K - p + 1$

The integral over the couple of steepest descent paths $\Gamma_{n,0} \cup \Gamma_{n,1}$ at every $t_n, n = 0, 1, \dots, K - p + 1$, is

$$F_n(x_1, \cdots, x_K) := \mathrm{e}^{\mathrm{i}|x_p|^{(K+2)\sigma} f(t_n)} |x_p|^{\sigma} \int_{\Gamma_{n,0} \cup \Gamma_{n,1}} \mathrm{e}^{\frac{\mathrm{i}}{2} f''(t_n)|x_p|^{(K+2)\sigma}(t-t_n)^2} g_n(x_1, \cdots, x_K; t) dt, \tag{23}$$

with

$$g_n(x_1, \dots, x_K; t) := \exp\left[\mathrm{i}|x_p|^{(K+2)\sigma}[f(t) - f_2^n(t)] + \mathrm{i} \sum_{m=1, m\neq p}^{K} x_m (|x_p|^{\sigma} t)^m \right], \tag{24}$$

$$t = t_n + e^{\mathrm{i}\theta_{n,0}} u, -\infty \leq u < \infty, \tag{25}$$

$$f_2^n(t) := f(t_n) + \frac{f''(t_n)}{2}(t - t_n)^2, \theta_{n,0} = \frac{\pi}{4} - \frac{K[\theta + (2n+1)\pi]}{2(K - p + 2)}. \tag{26}$$

Following Ref. 7, the asymptotic approximation of $F_n(x_1, \dots, x_K)$ for large $|x_p|$ is obtained after the change of variable $t \to t|x_p|^{-(K+2)\sigma/2}$, and replacing $g_n(x_1, \dots, x_K; t)$ by

$$g_n(x_1, \dots, x_K; t_n) = e^{\mathrm{i} \sum_{m=1, m\neq p}^{K} x_m (|x_p|^{\sigma} t_n)^m}. \tag{27}$$

Then,

$$F_n(x_1, \cdots, x_K) = \sqrt{\frac{2\pi i \sigma}{p(e^{i(2n+1)\pi} x_p)^{\sigma K}} \left(\frac{K+2}{p}\right)^{(p-2)\sigma}} \exp\left\{ i \sum_{m=1, m\neq p}^{K} x_m \left(\frac{p e^{i(2n+1)\pi} x_p}{K+2} \right)^{m\sigma} \right.$$
$$\left. - \frac{i}{(K+2)\sigma} \left(\frac{p}{K+2}\right)^{\sigma p} (e^{i(2n+1)\pi} x_p)^{(K+2)\sigma} \right\} \left[1 + \mathcal{O}\left(\frac{1}{x_p^{K\sigma}} \right) \right]. \tag{28}$$

5 | DEFORMATION OF THE PATH C_E OR C_O TO THE RELEVANT SADDLE POINTS AND STEEPEST DESCENT PATHS

In this section, we face the last step of the analysis: decide which ones are the relevant saddle points and the deformation of the original path C_o or C_e to the corresponding simplified steepest descent paths. We must deform the original integration path C_o or $C_e \to \Gamma$, where Γ is the union of several pieces of $\Gamma_{K+2-p,s}$ for certain values of s and/or a piece of $\Gamma_{n,0} \cup \Gamma_{n,1}$ for certain values $n = 0, 1, \dots, K - p + 1$, always containing the relevant saddle points.

When one of the relevant saddle points is a point t_n, $n = 0, 1, \dots, K - p + 1$, there is only one possible election of the union of simplified steepest descent paths through t_n: $\Gamma_{n,0} \cup \Gamma_{n,1}$. On the other hand, when $t = t_{K-p+2} = 0$ is also a relevant saddle point, we have to decide what couple of paths $\Gamma_{K+2-p,s}$ (what couple of values of s) we must take to go across the saddle point $t = 0$. In order to decide this, it is convenient to have some information about the location of the exact steepest descent paths of the phase function $f(t)$ at $t = 0$. Write $t = re^{i\varphi}, r > 0, -\pi < \varphi \leq \pi$.

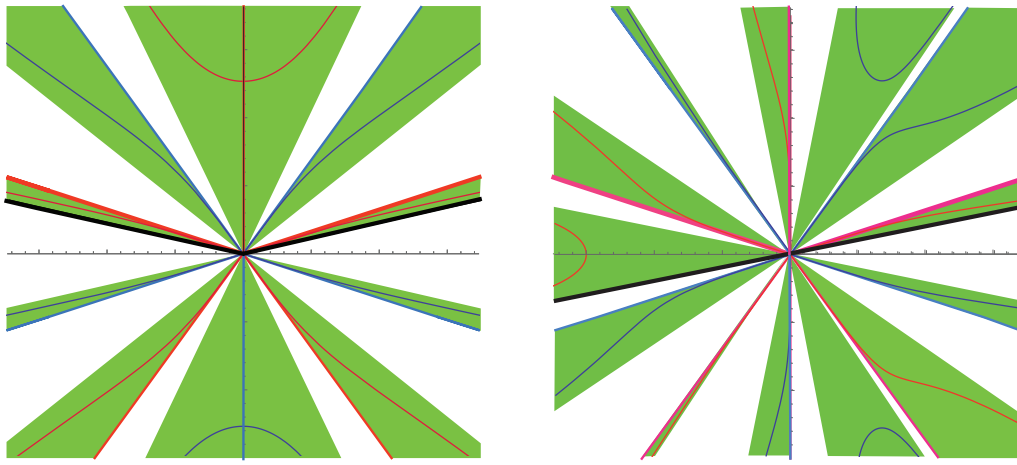

FIGURE 2 Left picture: $K = p = 5$ and $\theta = 0$. Right picture: $K = 6$, $p = 5$ and $\theta = 0$. Green sectors are the allowed sectors in the complex t plane defined by formula (29). Black straight lines are the original integration path C_o (left picture) or C_e (right picture). Red/blue straight lines are the simplified steepest descent/ascent paths at $t = 0$; the two thickest red ones are the relevant steepest descent straight lines, corresponding to $k = 0$ and $k = q$ in formula (31). The red/blue curves are the standard steepest descent/ascent paths at $t = 0$ of the standard saddle point method. All the curves are tangent, at the origin, to the simplified steepest descent/ascent straight lines; and at the infinity, to the borders of the green sectors given by formula (30).

The exact steepest ascent and descent paths $r(\varphi)$ at $t = 0$ satisfy $\Im[if(t)] = r^{K+2}\cos[(K+2)\varphi] + r^p\cos[p\varphi + \theta] = \Im[if(0)] = 0$, and therefore,

$$r^{K+2-p} = -\frac{\cos[p\varphi + \theta]}{\cos[(K+2)\varphi]}, \tag{29}$$

whenever the right-hand side is positive. This fact defines a set of allowed sectors in the complex t-plane where we can find the exact or standard steepest ascent and descent paths of the saddle point $t = 0$ and a complementary set of forbidden sectors. Figure 2 shows the allowed sectors for two particular examples of parameters (K, p). The asymptotes of these paths are some of the following angles:

$$\bar{\varphi}_k := \frac{2k+1}{K+2}\frac{\pi}{2}, k = 0, 1, 2, \cdots, 2K+3. \tag{30}$$

On the other hand, the exact steepest ascent and descent paths are tangent, at the origin, to the respective simplified steepest ascent and descent paths considered in our analysis. This means that, at $r = 0$, the exact steepest descent paths are tangent to the lines defined by the angles

$$\varphi_k := \frac{2k+1}{p}\frac{\pi}{2} - \frac{\theta}{p} = \theta_{K+2-p,k/2}, k = 0, 2, 4, \cdots, 2p-2, \tag{31}$$

with $\theta_{K+2-p,k/2}$ given in (17). Also, at $r = 0$, the exact steepest ascent paths are tangent to the lines defined by the angles

$$\varphi_k := \frac{2k+1}{p}\frac{\pi}{2} - \frac{\theta}{p}, k = 1, 3, 5, \cdots, 2p-1. \tag{32}$$

The original integration path is itself an asymptote, on the right-half t-plane, to the steepest descent path corresponding to $k = 0$, with angle $\bar{\varphi}_0$. And also, the original integration path is itself an asymptote, on the left-half t-plane, to the steepest descent path corresponding to $k = K + 2$, with angle $\bar{\varphi}_{K+2}$, if K is even, or to the steepest descent path corresponding to $k = K + 1$, with angle $\bar{\varphi}_{K+1}$, if K is odd.

Therefore, the relevant steepest descent paths at $t = 0$ are $\Gamma_{0,0}$ and $\Gamma_{0,q}$, q even, where the angle φ_q is the closest one to $\bar{\varphi}_{K+2}$ if K is even or $\bar{\varphi}_{K+1}$ if K is odd. This means that q is the even number $2n$ that minimizes

$$\left| \frac{(2n + 1/2)\pi - \theta}{p} - \frac{(2K + 4 + (-1)^K)\pi}{2(K + 2)} \right|, \tag{33}$$

that is,

$$q := \left\lfloor \left(1 + \frac{(-1)^K}{2K + 4} \right) p + \frac{\theta}{\pi} - \frac{1}{2} \right\rfloor. \tag{34}$$

Therefore, we may conclude that, when $|x_p| \to \infty$, and for a certain $n \in \{0, 1, \dots, K + 1 - p\}$,

$$\Psi_K \sim \begin{cases} F_n & \text{if only } t_n \text{ is relevant,} \\ F_0^0 - F_0^q & \text{if only } t = 0 \text{ is relevant,} \\ F_n + F_0^0 - F_0^q & \text{if both, } t_n \text{ and } t = 0, \text{ are relevant,} \end{cases} \tag{35}$$

where the asymptotic approximation of F_0^s and F_n is given in (22) and (28), respectively.

It only remains to determine which saddle points are relevant and then the corresponding deformation of the integration path C_o or $C_e \to \Gamma$, in order to decide which one of the three cases in (35) to take and the precise value of n. This becomes straightforward from formula (18), the above analysis in this section and Cauchy's residue theorem: when the saddle point $t_{K+2-p} = 0$ is dominant according to (18), then the path Γ must contain the simplified steepest descent paths $\Gamma_{K+2-p,0} \cup \Gamma_{K+2-p,q/2}$ defined by (13) and (17). When the saddle point t_n, $n = 0, 1, \dots, K + 1 - p$ is dominant according to (18), then the path Γ must contain the simplified steepest descent paths $\Gamma_{n,0} \cup \Gamma_{n,1}$ defined by (13) and (16).

It is clear from formula (18) that the particular value of n and then the deformation of the integration path depends on θ, but it turns out that it also depends on the even/odd character of K and p; moreover, the case $p = 1$ requires a separate analysis. Then, it is necessary to consider six possible cases separately: K even and $p = 1$, K odd and $p = 1$, K and p even, K even and $p > 1$ odd, K odd and p even (distinguishing the cases $2p < K + 2$ and $2p > K + 2$), and K and $p > 1$ odd. In the following subsections, we summarize the main details for each of the six cases: the relevant saddle points according to (18), and hence, the deformation of the original integration path C_o or $C_e \to \Gamma$. In every subsection, we illustrate the idea by means of two pictures: (i) the form of $\Re(f(t_n))$ with n given in formula (18) for general values of K and p and (ii) the form of the integration path Γ for certain examples of K and p, including the original integration path, and all the simplified steepest descent paths at every saddle point. Figures 3, 6, 9, 11, 14, 17, and 20 also indicate the dominant saddle point t_n in every asymptotic sector.

The asymptotic approximation of $\Psi_K(x_1, \dots, x_K)$ for large $|x_p|$ given below in formulas (36)–(37) follows from formulas (22) and/or (28), according to the presence of $\Gamma_{K+2-p,0} \cup \Gamma_{K+2-p,q/2}$ and/or $\Gamma_{n,0} \cup \Gamma_{n,1}$ in the deformed path Γ detailed in the following subsections and formula (35).

FIGURE 3 K even and $p = 1$

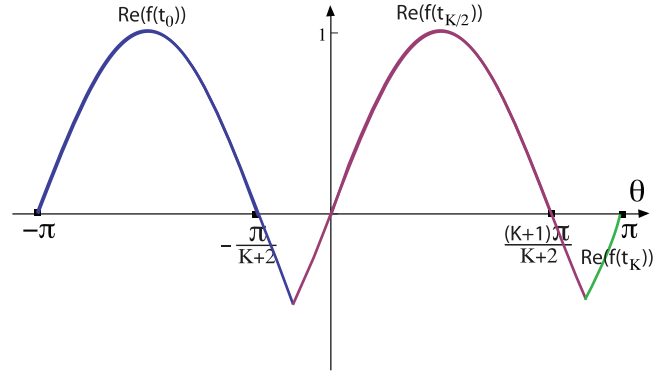

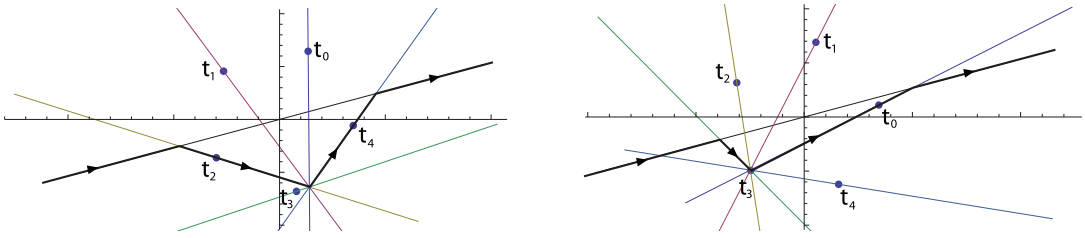

FIGURE 4 $\theta = 7\pi/8$ (left) and $\theta = -3\pi/4$ (right)

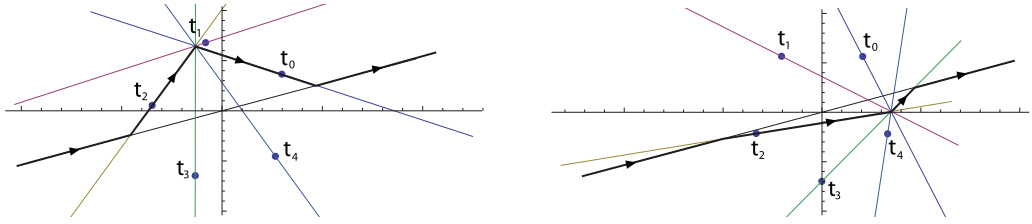

FIGURE 5 $\theta = -\pi/8$ (left) and $\theta = \pi/2$ (right)

5.1 | K even and $p = 1$

Figure 3 illustrates $\Re(f(t_n))$ with n given by formula (18) for K even and $p = 1$.

The dominant saddle points are:

- $t_0 = \dfrac{e^{i\sigma(\theta+\pi)}}{(K+2)^\sigma}$ for $-\pi < \theta \le -\dfrac{\pi}{2(K+2)}$.
- $t_{K/2} = \dfrac{e^{i\sigma[\theta+(K+1)\pi]}}{(K+2)^\sigma}$ for $-\dfrac{\pi}{2(K+2)} < \theta \le \dfrac{(2K+3)\pi}{2(K+2)}$.
- $t_K = \dfrac{e^{i\sigma[\theta+(2K+1)\pi]}}{(K+2)^\sigma}$ for $\dfrac{(2K+3)\pi}{2(K+2)} < \theta \le \pi$.

Figures 4 and 5 illustrate typical steepest descent paths for $K = 4$ and different values of θ.

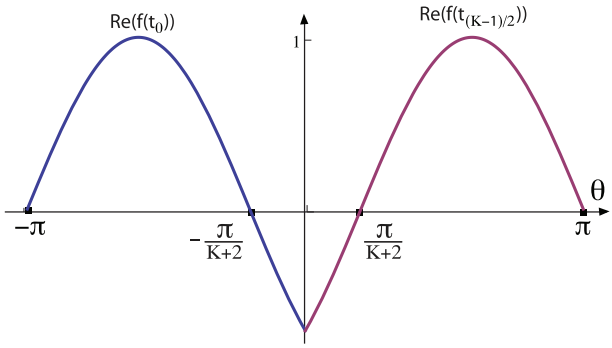

FIGURE 6 K odd and $p = 1$

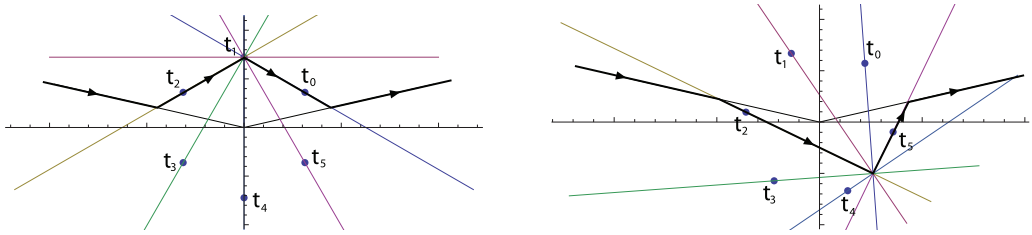

FIGURE 7 $\theta = 0$ (left) and $\theta = 3\pi/4$ (right)

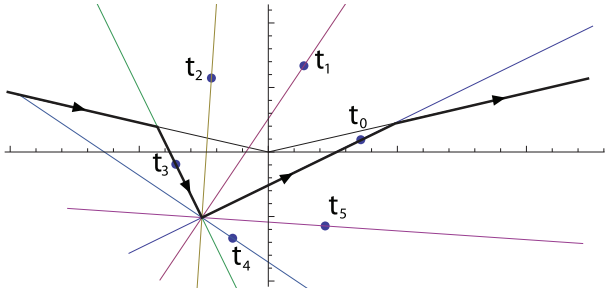

FIGURE 8 $\theta = -3\pi/4$

5.2 | K odd and $p = 1$

Figure 6 illustrates $\Re(f(t_n))$ with n given by formula (18) for K odd and $p = 1$. The dominant saddle points are

- t_0 for $-\pi < \theta \leq 0$.
- $t_{(K-1)/2}$ for $0 < \theta \leq \pi$.

Figures 7 and 8 illustrate typical steepest descent paths for $K = 5$ and different values of θ.

5.3 | K even and p even

Figure 9 illustrates $\Re(f(t_n))$ with n given by formula (18) for K and p even. The dominant saddle points are

FIGURE 9 K even and p even

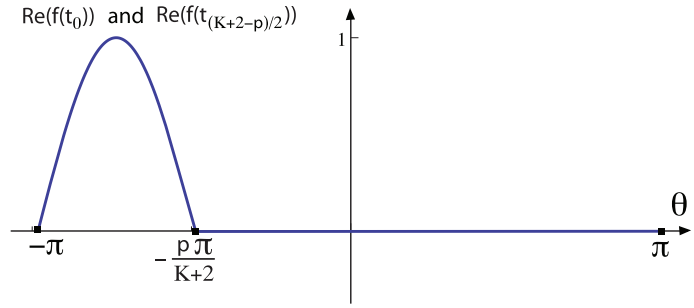

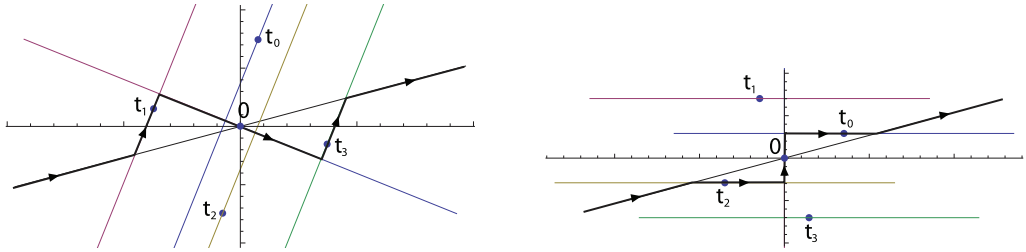

FIGURE 10 $\theta = 3\pi/4$ (left) and $\theta = -\pi/2$ (right)

FIGURE 11 K even and p odd

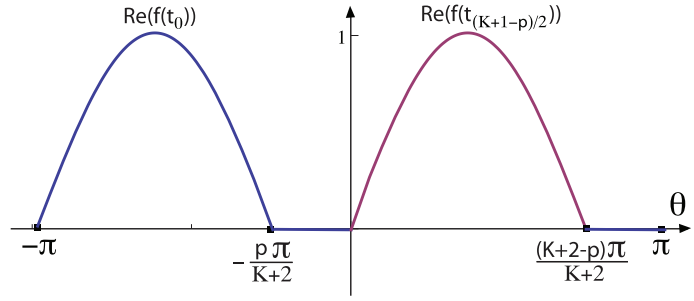

- t_0 and $t_{(K+2-p)/2}$ for $-\pi < \theta \leq -\frac{p\pi}{K+2}$.
- 0 for $-\frac{p\pi}{K+2} < \theta \leq \pi$.

Figure 10 illustrates typical steepest descent paths for $K = 4$, $p = 2$ and different values of θ.

5.4 | K even and p odd

Figure 11 illustrates $\Re(f(t_n))$ with n given by formula (18) for K even and p odd. The dominant saddle points are

- t_0 for $-\pi < \theta \leq -\frac{p\pi}{K+2}$.
- 0 for $-\frac{p\pi}{K+2} < \theta \leq 0$.
- $t_{(K+1-p)/2}$ for $0 \leq \theta \leq \frac{(K+2-p)\pi}{K+2}$.

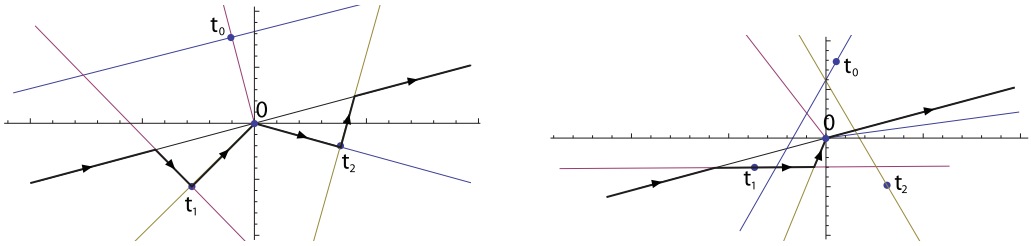

FIGURE 12 $\theta = 3\pi/4$ (left) and $\theta = 3\pi/8$ (right)

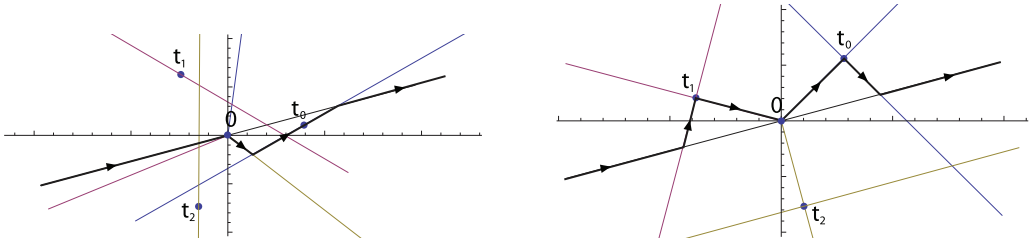

FIGURE 13 $\theta = -7\pi/8$ (left) and $\theta = -\pi/4$ (right)

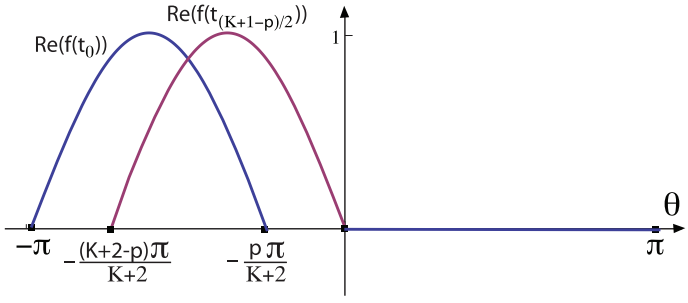

FIGURE 14 K odd and p even

- 0 for $\frac{(K+2-p)\pi}{K+2} < \theta \le \pi$.

Figures 12 and 13 illustrate typical steepest descent paths for $K = 4$, $p = 3$ and different values of θ.

5.5 | K odd and p even with $2p < K + 2$

Figure 14 illustrates $\Re(f(t_n))$ with n given by formula (18) for K odd and p even with $2p < K + 2$. The dominant saddle points are

- t_0 for $-\pi < \theta \le \frac{(p-K-2)\pi}{K+2}$.
- t_0 and $t_{(K+1-p)/2}$ for $\frac{(p-K-2)\pi}{K+2} \le \theta \le -\frac{p\pi}{K+2}$.
- $t_{(K+1-p)/2}$ for $-\frac{p\pi}{K+2} < \theta \le 0$.
- 0 for $0 \le \theta \le \pi$.

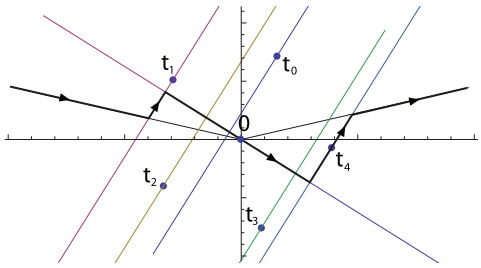

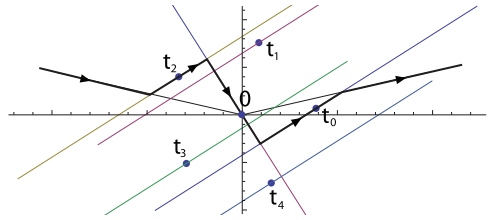

FIGURE 15 $\theta = 6\pi/7$ (left) and $\theta = -5\pi/7$ (right)

FIGURE 16 $\theta = -\pi/7$

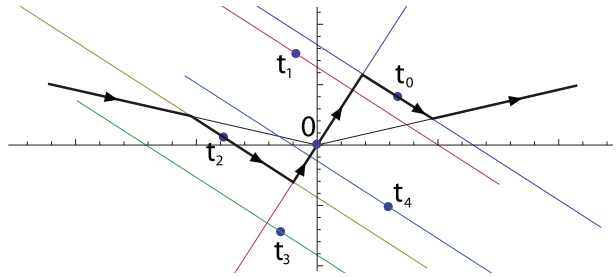

FIGURE 17 K odd and p even

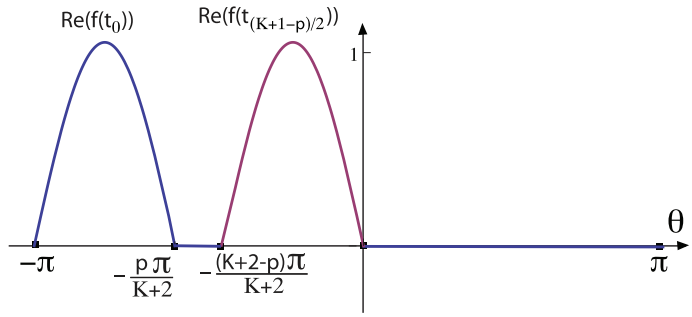

Figures 15 and 16 illustrate typical steepest descent paths for $K = 5$, $p = 2$ and different values of θ.

5.6 | K odd and p even with $2p > K + 2$

Figure 17 illustrates $\Re(f(t_n))$ with n given by formula (18) for K odd and p even with $2p > K + 2$. The dominant saddle points are

- t_0 for $-\pi < \theta \le -\frac{p\pi}{K+2}$.
- 0 for $-\frac{p\pi}{K+2} \le \theta \le \frac{(p-K-2)\pi}{K+2}$.
- $t_{(K+1-p)/2}$ for $\frac{(p-K-2)\pi}{K+2} \le \theta \le 0$.
- 0 for $0 \le \theta \le \pi$.

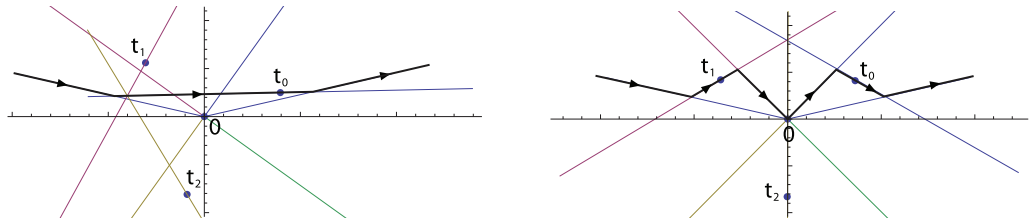

FIGURE 18 $\theta = -5\pi/7$ (left) and $\theta = -\pi/2$ (right)

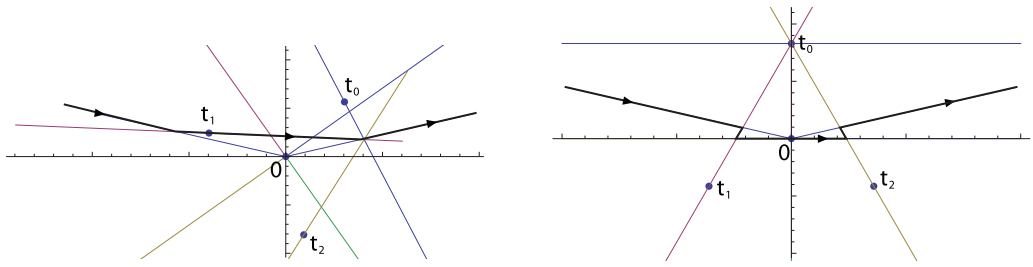

FIGURE 19 $\theta = -2\pi/7$ (left) and $\theta = \pi/2$ (right)

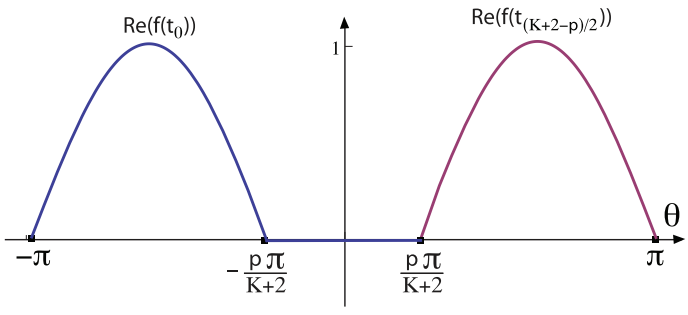

FIGURE 20 K and p odd

Figures 18 and 19 illustrate typical steepest descent paths for $K = 5$, $p = 4$ and different values of θ.

5.7 | K and p odd

Figure 20 illustrates $\Re(f(t_n))$ with n given by formula (18) for K and p odd. The dominant saddle points are

- t_0 for $-\pi < \theta \leq -\frac{p\pi}{K+2}$.
- 0 for $-\frac{p\pi}{K+2} \leq \theta \leq \frac{p\pi}{K+2}$.
- $t_{(K-p)/2}$ for $\frac{p\pi}{K+2} \leq \theta \leq \pi$.

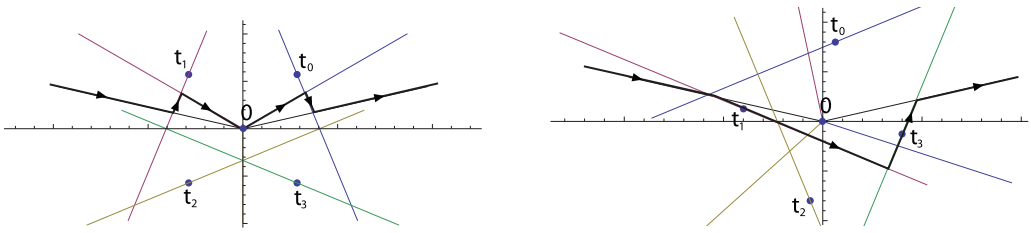

FIGURE 21 $\theta = 0$ (left) and $\theta = 4\pi/5$ (right)

FIGURE 22 $\theta = -4\pi/5$

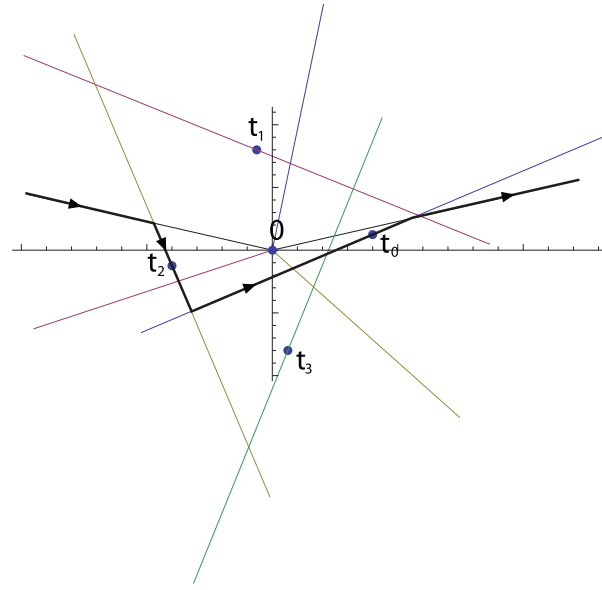

Figures 21 and 22 illustrate typical steepest descent paths for $K = 5$, $p = 3$ and different values of θ.

6 | ASYMPTOTIC APPROXIMATION OF $\Psi_K(x_1, \dots, x_K)$

In this section, we summarize the results of the above sections. Recall that only one variable, say x_p, is large and that we have written $x_p = |x_p|e^{i\theta}$, with $\theta := \arg x_p$. An asymptotic approximation of the family of the canonical catastrophe integrals $\Psi_K(x_1, \dots, x_K)$ for large $|x_p|$ is given in the following formula:

$$\Psi_K(x_1, \cdots, x_K) = \overline{\Psi}_K(x_1, \cdots, x_K)\left[1 + \mathcal{O}\left(\frac{1}{x_p^{\gamma}}\right)\right], |x_p| \to \infty, \tag{36}$$

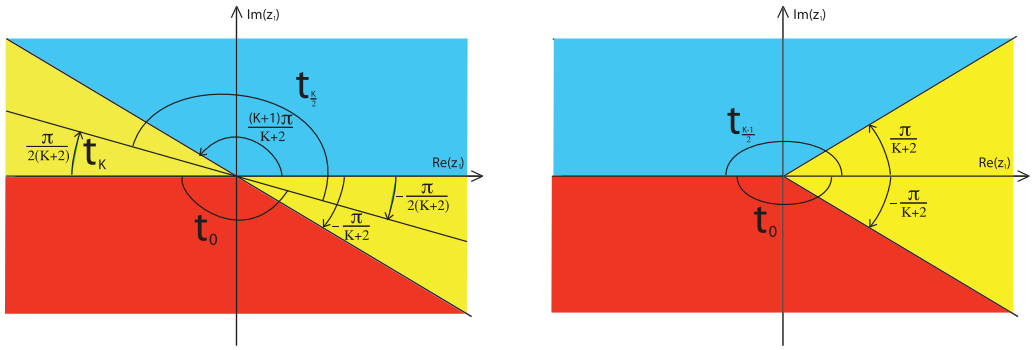

FIGURE 23 Left picture: K even and $p = 1$. Right picture: K odd and $p = 1$

where the elementary function $\bar{\Psi}_K(x_1, \dots, x_K)$ that encodes the asymptotic behavior of $\Psi_K(x_1, \dots, x_K)$ is

$$\bar{\Psi}_K(x_1, \dots, x_K) := \begin{cases} \sqrt{\dfrac{2\pi i\sigma}{p(e^{i\pi\beta}x_p)^{\sigma K}}\left(\dfrac{K+2}{p}\right)^{(p-2)\sigma}} \exp\left\{ i \displaystyle\sum_{m=1, m\neq p}^{K} x_m \left(\frac{e^{i\pi\beta}x_p}{K+2}\right)^{m\sigma} \right. \\ \qquad \left. - \dfrac{i}{(K+2)\sigma}\left(\dfrac{p}{K+2}\right)^{\sigma p}(e^{i\pi\beta}x_p)^{(K+2)\sigma} \right\}, \quad \theta \in R_e, \\ \dfrac{\Gamma\left(1+\frac{1}{p}\right)}{x_p^{1/p}} e^{i\pi/(2p)}\left(1 - e^{i\pi q/p}\right), \quad \theta \in R_p. \end{cases} \tag{37}$$

The parameters involved in the above formulas are:

$$\sigma := \frac{1}{K+2-p}, \tag{38}$$

$$\gamma := \begin{cases} \dfrac{K}{K+2-p} & \text{for } \theta \in R_e, \\ \dfrac{1}{p} & \text{for } \theta \in R_p, \end{cases} \tag{39}$$

$$q := \left\lfloor \left(1 + \frac{(-1)^K}{2K+4}\right)p + \frac{\theta}{\pi} - \frac{1}{2} \right\rfloor, \tag{40}$$

where the symbol $\lfloor x \rfloor$ stands for the even number closest to x. The values of the parameter β and the sectors R_e, R_p in formula (37), together the corresponding Stokes lines of the asymptotic approximation (36)–(37), are given in Table 1. The catastrophe integral $\Psi_K(x_1, \dots, x_K)$ has a power behavior in the regions R_p (green) and an exponential behavior in the regions R_e (yellow for negative exponential behavior and blue or red for positive exponential behavior).

The different asymptotic regions R_e and R_p and the corresponding Stokes lines encoded in formulas (36)–(37) and Table 1 are summarized in Figures 23–26.

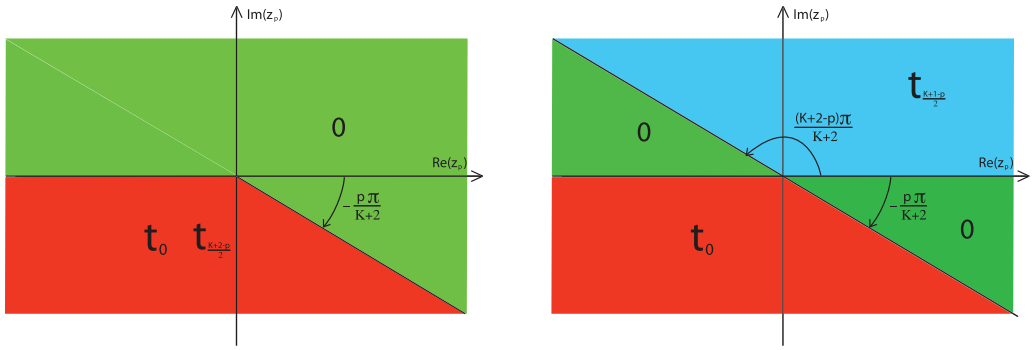

FIGURE 24 Left picture: K even and p even. Right picture: K even and $p \neq 1$ odd

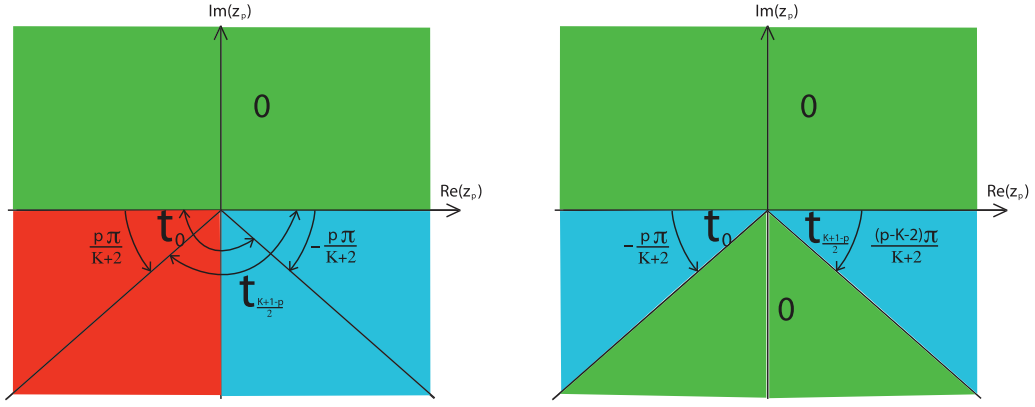

FIGURE 25 K odd and p even. Left picture: $2p < K + 2$. Right picture: $2p > K + 2$

FIGURE 26 K odd and $p \neq 1$ odd

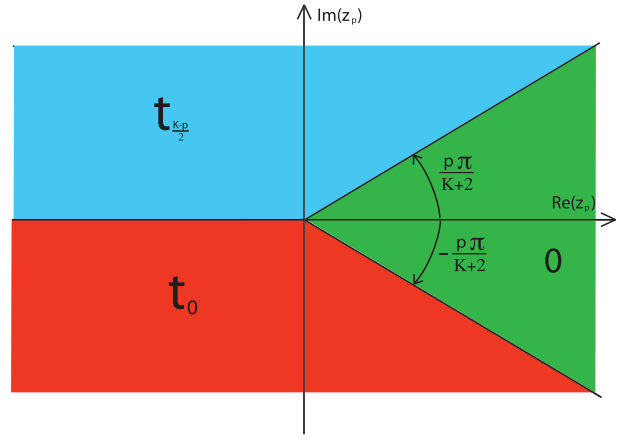

7 | NUMERICAL EXPERIMENTS

In Tables 2–8, we give some numerical experiments (relative error) that illustrate the approximation given by formulas (36)–(37) and Table 1, for every one of the seven different (K, p) regions

TABLE 2 K even and $p = 1$

	$K = 2$ $\mathbf{x} = (x_1, 0.1)$			$K = 4$ $\mathbf{x} = (x_1, 0.1, 0.05e^{i\frac{\pi}{6}}, -0.1)$				$K = 6$ $\mathbf{x} = (x_1, 0.1, 0.05e^{i\frac{\pi}{6}}, -0.1, 0.02, 0.1)$			
$\lvert x_1\rvert$ \ $\arg x_1$	$-\frac{\pi}{2}$	$\frac{\pi}{3}$	$\frac{7.5\pi}{8}$	$\lvert x_1\rvert$ \ $\arg x_1$	$-\frac{\pi}{4}$	0	$\frac{11.5\pi}{12}$	$\lvert x_1\rvert$ \ $\arg x_1$	$-\frac{\pi}{4}$	0	$\frac{15.5\pi}{16}$
10	0.02	0.012	0.02	10	0.04	0.03	0.07	30	0.02	0.01	0.01
30	0.007	0.007	0.002	50	0.006	0.002	0.004	100	0.016	0.001	0.008

TABLE 3 K odd and $p = 1$

	$K = 3$ $\mathbf{x} = (x_1, 0.5e^{i\frac{\pi}{6}}, 0.2i)$		$K = 5$ $\mathbf{x} = (x_1, 0.1, 0.05, -0.1, 0.02)$			$K = 7$ $\mathbf{x} = (x_1, 0.1, -0.2, i, 0.3, 0, 0.05)$		
$\lvert x_1\rvert$ \ $\arg x_1$	$-\frac{4\pi}{5}$	$\frac{3\pi}{4}$	$\lvert x_1\rvert$ \ $\arg x_1$	$-\frac{\pi}{2}$	$\frac{\pi}{2}$	$\lvert x_1\rvert$ \ $\arg x_1$	$-\frac{\pi}{4}$	$\frac{\pi}{4}$
10	0.1	0.02	10	0.045	0.05	0.5	0.3	0.3
100	0.05	0.009	100	0.002	0.01	10	0.1	0.2

TABLE 4 K even and p even

	$K = 4, p = 2$ $\mathbf{x} = (0.1, x_2, 0.05e^{i\frac{\pi}{6}}, -0.01)$			$K = 4, p = 4$ $\mathbf{x} = (0.1, 0.02, 0.05e^{i\frac{\pi}{6}}, x_4)$			$K = 6, p = 2$ $\mathbf{x} = (0.1, x_2, 0.05e^{i\frac{\pi}{6}}, -0.1, 0.02, 0.1)$		
$\lvert x_2\rvert$ \ $\arg x_2$	$-\frac{\pi}{2}$	0	$\lvert x_4\rvert$ \ $\arg x_4$	$-\frac{5\pi}{4}$	0	$\lvert x_4\rvert$ \ $\arg x_4$	$-\frac{3\pi}{5}$	0
5	0.6	0.02	10	0.005	0.009	5	0.6	0.03
30	0.5	1.e-4	100	0.001	8.e-4	20	0.5	1.e-4

TABLE 5 K even and $p \neq 1$ odd

	$K = 4, p = 3$ $\mathbf{x} = (0.1, 0.02, x_3, 0.05e^{i\frac{\pi}{6}})$				$K = 6, p = 5$ $\mathbf{x} = (0.1, -0.02, 0.05e^{i\frac{\pi}{6}}, -0.1, x_5, 0.1)$				
$\lvert x_3\rvert$ \ $\arg x_3$	$-\frac{4\pi}{5}$	$\frac{3\pi}{4}$	$-\frac{\pi}{2}$	$\frac{\pi}{2}$	$\lvert x_5\rvert$ \ $\arg x_5$	$-\frac{7\pi}{8}$	$-\frac{\pi}{2}$	$\frac{\pi}{8}$	$\frac{7\pi}{8}$
10	0.02	0.02	0.02	0.03	0.5	0.3	0.2	0.1	0.14
100	0.017	0.01	0.016	0.01	10	0.07	0.01	0.06	0.024

TABLE 6 K odd and p even with $2p < K + 2$

	$K = 3, p = 2$ $\mathbf{x} = (0.1, x_2, 0.2)$				$K = 5, p = 2$ $\mathbf{x} = (0.1, x_2, 0.05e^{i\frac{\pi}{6}}, -0.01, 0.)$				
$\lvert x_2\rvert$ \ $\arg x_2$	$-\frac{4\pi}{5}$	$-\frac{\pi}{2}$	$-\frac{\pi}{5}$	$\frac{\pi}{3}$	$\lvert x_2\rvert$ \ $\arg x_2$	$-\frac{6\pi}{7}$	$-\frac{4\pi}{7}$	$-\frac{\pi}{2}$	$\frac{\pi}{4}$
10	0.04	0.6	0.04	6.e-4	10	0.04	0.05	0.03	2.e-4
30	0.03	0.5	0.03	1.e-4	30	0.008	0.008	0.007	8.e-5

TABLE 7 K odd and p even with $2p > K + 2$

		$\boldsymbol{K = 5, p = 4}$ $\mathbf{x} = (\mathbf{0.5}, \mathbf{0.01}, \mathbf{-0.3}, \boldsymbol{x_4}, \mathbf{0})$	
$\lvert x_4\rvert \diagdown \arg x_4$	$-\frac{6\pi}{7}$	-1	$\frac{\pi}{4}$
8	0.005	0.005	0.01
15	0.004	0.004	0.009

TABLE 8 K odd and $p \neq 1$ odd

			$\boldsymbol{K = 3, p = 3}$ $\mathbf{x} = (\mathbf{0.1}, \mathbf{0.2}, \boldsymbol{x_3})$			$\boldsymbol{K = 5, p = 3}$ $\mathbf{x} = (\mathbf{0.1}, \mathbf{-0.02}, \boldsymbol{x_3}, \mathbf{0.1}, \mathbf{0.05e}^{\boldsymbol{i}\frac{\pi}{6}})$		
$\lvert x_3\rvert \diagdown \arg x_3 4$	$-\frac{\pi}{2}$	0	$\frac{4\pi}{5}$	$\lvert x_3\rvert \diagdown \arg x_3$	$-\frac{\pi}{2}$	0	$\frac{\pi}{2}$
5	0.03	0.03	0.03	10	0.02	0.02	0.06
10	0.02	0.02	0.005	30	0.016	0.016	0.03

detailed in Table 1 and several values of the asymptotic parameter x_p and the other parameters $x_k, k \neq p$.

Observe that when $|x_1|$ increases from 10 to 100 in the leftmost table in Table 3, the relative error only decreases around 50%. Numerical experiments are more or less satisfactory depending on different factors. From formula (15), we deduce that there is a constant $M > 0$ (which depends on $\arg x_1$ and the other parameters x_k) such that |relative error| $\leq M|x_p^{-\gamma}|$ for large enough $|x_p|$. Therefore, the larger $|x_p|$ is, the lower the relative error bound $M|x_p^{-\gamma}|$ is. We may expect a similar behavior of the actual relative error, but it strongly depends on the (unknown) constant M.

Taking a closer look to Table 3, for $K = 3$, we have that $\gamma = 3/4$ with $R_e = (-\pi, \pi]$ and $R_p = \phi$. Then, the relative error is bounded by $M \times 0.1778$ for $|x_1| = 10$ and by $M \times 0.0316$ for $|x_1| = 100$. The larger $|x_p|$ is, the lower the relative error bound is. But, although we may expect a reduction of the relative error in a similar proportion, we cannot assure that precise reduction for the relative error, but only an estimation. Then, it is possible that the relative error decreases only around 50%, whereas $|x_1|$ increases 10 times.

On the other hand, observe that for other arguments of the large variable x_1, farther away from the Stokes lines (the arguments in the leftmost table in Table 3 are not very far), the relative error is smaller and decreases faster when $|x_1|$ increases. In other words, it is reasonable to expect that the unknown constant M strongly depends on $\arg x_1$.

More satisfactory numerical results would be obtained by computing more terms of the asymptotic expansions. This is subject of further investigation.

ACKNOWLEDGMENTS

This research was supported by the *Universidad Pública de Navarra*, research grant PRO-UPNA (6158) 01/01/2022.

DATA AVAILABILITY STATEMENT

Data sharing not applicable to this article as no datasets were generated or analysed during the current study.

ORCID

José L. López https://orcid.org/0000-0002-6050-9015

REFERENCES

1. Berry MV, Howls CJ. Integrals with coalescing saddles. In: *NIST Handbook of Mathematical Functions*, Chapter 36. Cambridge University Press; 2010:775-793.
2. Connor JNL, Kurtis PR. A method for the numerical evaluation of the oscillatory integrals associated with the cuspoid catastrophes: application to Pearcey's integral and its derivatives. *J Phys A*. 1982;15(4):1179-1190.
3. Ferreira C, López JL, Pérez Sinusía E. The asymptotic expansion of the swallowtail integral in the highly oscillatory region. *Appl Math Comput*. 2018;339:837-845.
4. Ferreira C, López JL, Pérez Sinusía E. The swallowtail integral in the high oscillatory region II. *Electron Trans Numer Anal*. 2020;52:88-99.
5. Ferreira C, López JL, Pérez Sinusía E. The swallowtail integral in the highly oscillatory region III. *Complex Var Elliptic Equ*. 2022;67(5):1262-1272. https://doi.org/10.1080/17476933.2020.1868447
6. López JL, Pagola P. Convergent and asymptotic expansions of the Pearcey integral. *J Math Anal Appl*. 2015;430(1):181-192.
7. López JL, Pagola P, Pérez Sinusía E. A systematization of the saddle point method. Application to the Airy and Hankel functions. *J Math Anal Appl*. 2009;354(1):347-359.
8. Lord Kelvin. Deep water ship-waves. *Philos Mag*. 1905;9:733-757.
9. Olde Daalhuis AB. On the asymptotics for late coefficients in uniform asymptotic expansions of integrals with coalescing saddles. *Methods Appl Anal*. 2000;7(4):727-745.
10. Paris RB. The asymptotic behaviour of Pearcey's integral for complex variables. *Proc Roy Soc London Ser A*. 1991;432(1886):391-426.
11. Ursell F. Integrals with a large parameter. Several nearly coincident saddle points. *Proc Camb Philos Soc*. 1972;72:49-65.
12. Ursell F. *Ship Hydrodynamics, Water Waves and Asymptotics*, Collected Papers of F. Ursell, 1946–1992, Vol. 2. World Scientific Publishing Co; 1994.
13. Wong R. *Asymptotic Approximations of Integrals*. Academic Press; 1989.

How to cite this article: Ferreira C, López JL, Pérez Sinusía E. Asymptotic approximation of a highly oscillatory integral with application to the canonical catastrophe integrals. *Stud Appl Math*. 2023;150:254–276. https://doi.org/10.1111/sapm.12539